ACTIVE CONTROL OF FREE AND IMPINGING JETS FOR MODIFICATION OF MIXING

Jungwoo Kim
School of Mechanical and Aerospace Engineering,
Seoul National University

Jeongyoung Park
Applied Technology Research Department,
Hyundai Mobis

Haecheon Choi
School of Mechanical and Aerospace Engineering,
Seoul National University
choi@socrates.snu.ac.kr

ABSTRACT

The objective of the present study is to modify the mixing and heat transfer in turbulent free and impinging jets using an active control method, where the jet-exit Reynolds number is 10,000. As an active control method, time-periodic blowing and suction is applied at the jet exit. The excitation frequency is selected to be $St_\theta = 0.017$ corresponding to the maximum growth rate in the mixing layer, where θ is the momentum thickness at the jet exit. First, in free jet, the modification of vortical structures due to the excitation results in turbulence suppression in a downstream location. Accordingly, mixing is reduced in a downstream location as compared with that without excitation. Secondly, in impinging jet, the effect of excitation significantly depends on the distance (H) between the jet exit and the wall. In the present study, $H/D = 2$, 6 and 10 are considered to investigate this effect, where D is the jet diameter. The heat transfer rate at the wall is enhanced due to the excitation in the cases of $H/D = 2$ and 6. On the other hand, the heat transfer rate in the case of $H/D = 10$ decreases as compared with that without excitation. These results are related to the changes in vortical structures by the excitation.

INTRODUCTION

Many researchers have investigated turbulent free and impinging jets for understanding their mixing properties and heat transfer characteristics. Generally, the development of vortical structures has a close relation with the mixing and heat transfer characteristics. Therefore, quite a few active and passive control methods that result in turbulence suppression or enhancement have been applied to these flows in order to control mixing and heat transfer (Crow and Champagne 1971; Zaman and Hussain 1980, 1981). Especially, Zaman and Hussain (1981) observed that turbulence in a jet flow significantly changes when the jet is acoustically excited at a single frequency near the natural shear layer frequency of $St_\theta = 0.012$ based on the initial shear layer momentum thickness (θ). They observed that turbulence suppression occurs in the range of $0.01 < St_\theta < 0.02$ and maximum turbulence suppression in the jet flow occurs at $St_\theta = 0.017$ which corresponds to the maximum growth rate in the mixing layer (Michalke 1965). As a result, the mixing properties such as the mean axial velocity were changed significantly because the evolution of vortical structures was changed by the excitation. Similarly, Tong and Warhaft (1994) and Rajagopalan and Antonia (1998) observed that turbulence suppression occurs when a ring or a circular cylinder is located inside the shear layer.

On the other hand, the vortical structures in impinging jet evolve differently with H/D, and the heat transfer characteristics are affected by the vortical structures developed from the jet exit. For example, two local peaks of the Nusselt number exist in the case of $H/D = 2$, whereas only one peak exists in the cases of $H/D = 6$ and 10. Also, the Nusselt number at the stagnation point is largest in the case of $H/D = 6$ because of large turbulent intensity at this parameter (Lee and Lee 1999). Therefore, the effect of excitation may significantly depend on H/D. Liu and Sullivan (1996) performed single-frequency excitations for the cases of small H/D. Hwang and Cho (2003) investigated the effects of excitation frequency St_D and H/D on the Nusselt number and showed that the change in the Nusselt number due to the excitation is different for different H/D.

The objective of the present study is to apply a time-periodic excitation to turbulent free and impinging jets for mixing modification. The excitation frequency used is $St_\theta = 0.017$ that corresponds to the maximum growth rate in the mixing layer. The effect of excitation on vortical structures and mixing property is investigated in the free and impinging jets. For impinging jet, we also consider the effect of H/D on the Nusselt number.

NUMERICAL METHODS

The governing equations of unsteady incompressible viscous flow are

$$\frac{\partial u_i}{\partial t} + \frac{\partial u_i u_j}{\partial x_j} = -\frac{\partial p}{\partial x_i} + \frac{1}{\mathrm{Re}} \frac{\partial^2 u_i}{\partial x_j \partial x_j}, \tag{1}$$

$$\frac{\partial u_i}{\partial x_i} = 0, \tag{2}$$

$$\frac{\partial \theta}{\partial t} + \frac{\partial u_j \theta}{\partial x_j} = \frac{1}{\mathrm{RePr}} \frac{\partial^2 \theta}{\partial x_j \partial x_j}, \tag{3}$$

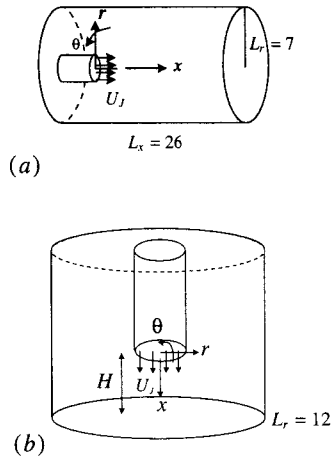

Figure 1: Schematic diagrams of (a) free jet; (b) impinging jet.

where x_i's are the cylindrical coordinates, u_i's are the corresponding velocity components, p is the pressure, and θ is the temperature. In the present study, turbulent flow is simulated using the large eddy simulation technique with a dynamic subgrid-scale model (Germano *et al.* 1991; Lilly 1992). The governing equations for large eddy simulation are obtained from the filtering operation for the continuity, momentum and energy equations.

The numerical scheme to solve the filtered unsteady three-dimensional Navier-Stokes and energy equations in the cylindrical coordinates is based on a semi-implicit fractional-step method used by Akselvoll and Moin (1995). The computational domain is decomposed into core and outer regions. Within each region only the derivatives in one direction are treated implicitly, i.e. derivatives in the azimuthal direction within the core region and derivatives in the radial direction within the outer region. The Crank-Nicolson method is used for the implicit terms and a 3rd-order Runge-Kutta method is used for the explicit terms. The convection term in the energy equation is discretized using the monotone difference scheme (Koren 1993) to avoid nonphysical wiggles in the temperature field, and all other terms are discretized with the 2nd-order central difference scheme in space.

Free jet

Figure 1(a) shows the schematic diagram of the computational domain used for the free jet. For the velocity components, the Neumann condition is used at the outflow boundary and the inflow boundary except the jet exit. At the lateral boundary, $\partial r u_r/\partial r = 0$ and $\omega_x = \omega_\theta = 0$ are used, where ω_x and ω_θ are the streamwise and azimuthal vorticity components. Thus, the ambient fluid is entrained from the inflow boundary as well as from the lateral boundary. Also, for the temperature, the convective boundary condition is used at the outflow boundary and the Neumann condition is used at the lateral boundary and at the inflow boundary except the jet exit. At the jet exit, we impose a top-hat velocity with a Blasius profile near the wall and a uniform temperature profile. The momentum thickness normalized by the jet diameter is $D/\theta = 120$.

The computational domain size is $-3.6 < x/D < 22.4$ and $0 < r/D < 7$. The numbers of grid points used are

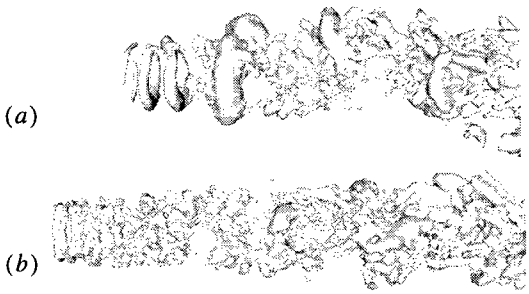

Figure 2: Instantaneous vortical structures (iso-pressure surfaces, $p = -0.03$) in the free jet: (a) without control; (b) with control.

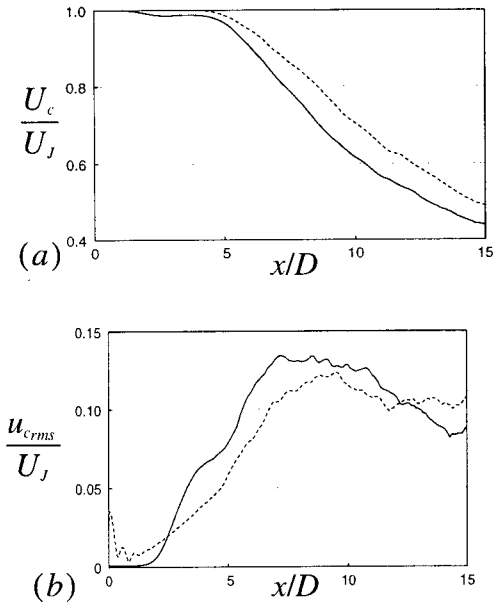

Figure 3: (a) Mean axial velocity along the centerline; (b) rms axial velocity fluctuations along the centerline. ——, Without control; – – – –, with control.

288 (x) × 96 (r) × 96 (θ) in the streamwise, radial, and azimuthal directions, respectively. To resolve the Blasius profile near the jet exit, nine grid points are located inside the boundary layer.

The velocity in (1) and (2) is normalized with the jet exit velocity U_J. The temperature in (3) is nondimensionalized as $(\theta - \theta_\infty)/(\theta_J - \theta_\infty)$, where θ_∞ and θ_J are the ambient fluid temperature and jet exit temperature, respectively. The Reynolds number based on the jet diameter and jet exit velocity is 10,000. In the present study, air is considered as the working fluid so that the Prandtl number is 0.71.

Impinging jet

Figure 1(b) shows the schematic diagram of the computational domain for the impinging jet. For the velocity components and temperature, the Neumann condition is used at the lateral boundary and the inflow boundary except the jet exit. At the jet exit, a top-hat velocity with a Blasius profile is specified, and a uniform temperature profile is specified. At the wall, no-slip boundary condition is used for the velocity and the uniform heat flux condition is applied at the wall.

In the present study, three cases of $H/D = 2, 6$ and 10 are

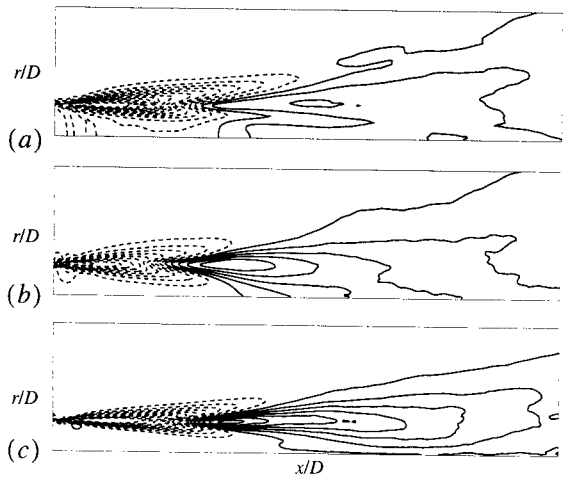

Figure 4: Changes in the Reynolds stresses due to the excitation: (a) contours of $u'_{un} - u'_{con}$ from -0.17 to 0.03; (b) contours of $v'_{un} - v'_{con}$ from -0.13 to 0.07; (c) contours of $u'v'_{un} - u'v'_{con}$ from -0.01 to 0.007. Here, the subscripts 'un' and 'con' denote the uncontrolled and controlled flows, respectively. Negative contours are dashed and the domain shown is $0 < x/D < 8$ and $0 < r/D < 2$.

considered. The computational domain size is $-16 < x/D < H/D$ and $0 < r/D < 12$. The numbers of grid points used are 136 $(x) \times 311$ $(r) \times 120$ (θ), 200 $(x) \times 304$ $(r) \times 120$ (θ) and 200 $(x) \times 304$ $(r) \times 120$ (θ), respectively, for $H/D = 2$, 6 and 10.

The velocity in (1) and (2) is normalized with U_J and the temperature in (3) is nondimensionalized as $(\theta_J - \theta)/(q''D/k)$, where θ_J and q'' are the jet exit temperature and heat flux at the wall. The Reynolds number and Prandtl number used for the impinging jet are the same as those for the free jet.

RESULT

In this study, we impose a single-frequency excitation at the jet exit as an active control. That is, the jet exit velocity is prescribed as $u(r,t)|_{jet\ exit} = U_J(r) \times [1 + A\sin(2\pi ft)]$, where the non-dimensional excitation frequency is $St_\theta = f\theta/U_J = 0.017$, the excitation amplitude is $A = 0.05$ and U_J is the maximum value of $U_J(r)$. Here, $U_J(r)$ is the exit velocity profile in the uncontrolled case.

Free jet

Figure 2 shows the instantaneous vortical structures without and with the excitation, where the surfaces of vortical structures are identified by the pressure. In the uncontrolled case (Fig. 2a), the shear layer becomes unstable due to the Kelvin-Helmholtz instability and vortex roll-up and their merging are observed. Large coherent structures are also observed due to the merging. On the other hand, in the controlled case (Fig. 2b), the shear layer becomes unstable right after the jet exit and the vortical structures are saturated at a much earlier position than those in the uncontrolled case. As a result, the vortices break down into fine-grained turbulence in a downstream location, which significantly reduces turbulence there. This phenomenon agrees well with that by Zaman and Hussain (1981).

Figure 3 shows the mean axial velocity (U_c) and rms axial velocity fluctuations (u_{crms}) without and with the excitation. The jet-centerline velocity decreases in the axial

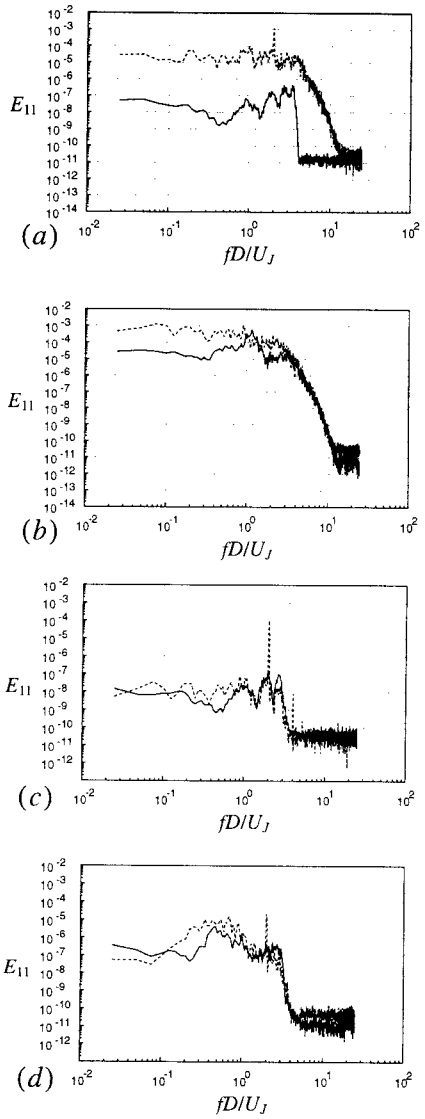

Figure 5: Energy spectra of the axial velocity (E_{11}): (a) $x/D = 0.5$ and $r/D = 0.4$; (b) $x/D = 2$ and $r/D = 0.4$; (c) $x/D = 0.5$ and $r/D = 0$; (d) $x/D = 2$ and $r/D = 0$. ——, Without control; – – – –, with control.

direction due to mixing. In the controlled case, the mean axial velocity decreases more slowly than that in the uncontrolled case. Therefore, mixing in the controlled case is smaller than that in the uncontrolled case. The reduction of mixing in the controlled case is caused by the fact that large coherent structures, which have an important role in mixing, break down into fine-grained turbulence due to the excitation (Fig. 2). In addition, the shear layer in the vicinity of the jet exit grows more rapidly in the controlled case than in the uncontrolled case as shown in Fig. 2. Accordingly, as shown in Fig. 3(b), the early development of the shear layer due to the excitation results in the increase in the rms axial velocity fluctuations near the jet exit. However, at $x/D > 2.5$, they become smaller than those in the uncontrolled case and the maximum value due to the excitation is reduced by about 8 %. Zaman and Hussain (1981) reported turbulence suppression by 9 % and Tong and Warhaft (1994) obtained turbulence suppression by 30 %. Furthermore, the axial location for the maximum turbulence intensity moves from $x/D = 7$ to $x/D = 9.5$ (see Fig. 3(b)).

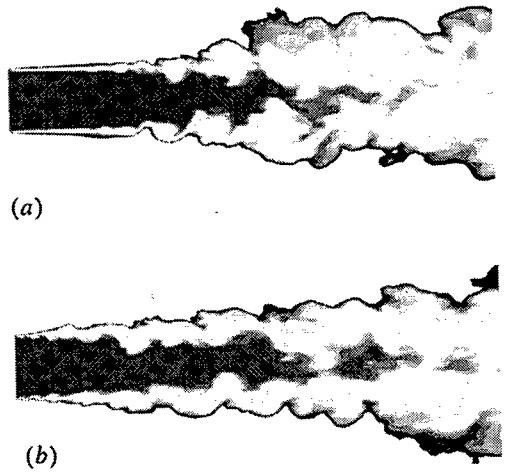

Figure 6: Contours of the instantaneous temperature in the free jet: (a) without control; (b) with control.

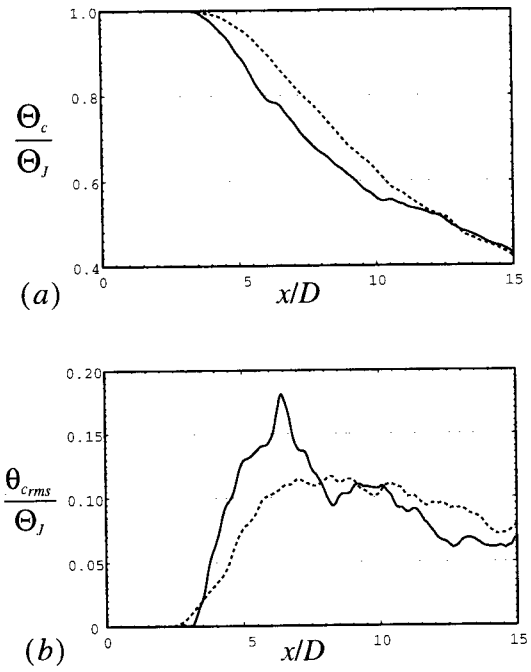

Figure 7: (a) Mean temperature along the centerline; (b) rms temperature fluctuations along the centerline. ——, Without control; – – – –, with control.

The changes in the axial and radial velocity fluctuations and Reynolds shear stress due to the excitation are shown in Fig. 4. The positive value indicates the region where turbulence suppression occurs due to the excitation. For all the Reynolds stresses, the values in the controlled case are higher than those in the uncontrolled case up to $x/D = 2$. These increases in the Reynolds stresses are due to the rapid increase in the shear layer instability. At further downstream locations ($x/D > 2$), the Reynolds stresses in the controlled case decrease as compared with those in the uncontrolled case. Noticeably, the changes in the Reynolds stresses occur mainly along the shear layer rather than along the centerline, confirming that the present forcing indeed triggers the shear layer instability.

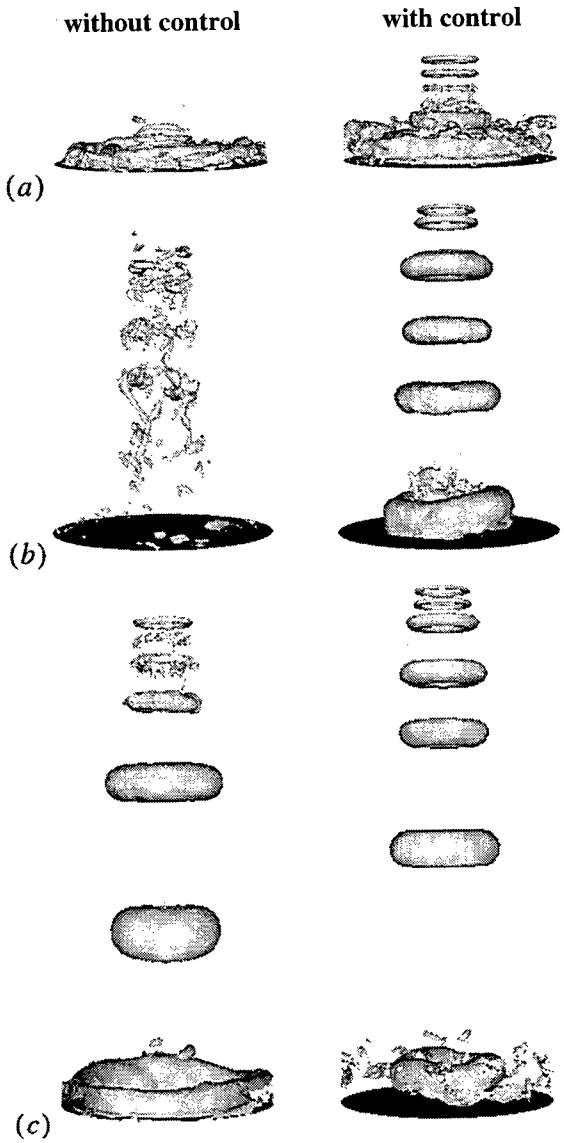

Figure 8: Instantaneous vortical structures (iso-pressure surfaces): (a) $H/D = 2$; (b) 6; (c) 10. Iso-pressure values are -0.07 for (a) and (b) and -0.1 for (c), respectively.

Generally, the jet flow has two instability modes: the shear layer mode and the jet column mode (Ho and Huerre 1984). To investigate how the excitation frequency used in the present study interacts with these instability modes, the energy spectra for the axial velocity at $r/D = 0.4$ and 0 are shown in Fig. 5, together with those without excitation. With the excitation, at $x/D = 0.5$ (Figs. 5(a) and (c)), a single peak is observed at the forcing frequency of $St_\theta = 0.017$ ($St_D = St_\theta D/\theta = 2.04$). However, the energy spectrum at $x/D = 2$ is already broad-band in the shear layer as compared with that without excitation (Fig. 5(b)). Therefore, it confirms that the excitation at $St_\theta = 0.017$ produces fined-grained turbulence in the downstream. On the other hand, the energy spectrum with the excitation does not change into a broad-band one at the centerline (Fig. 5(d)), indicating that the present excitation interacts strongly with the shear layer mode rather than the jet column mode.

Figure 6 shows the instantaneous temperature contours without and with the excitation. Again, it is clear that the initial shear layer becomes more unstable with the excitation and thus the thickness of the shear layer is larger in the

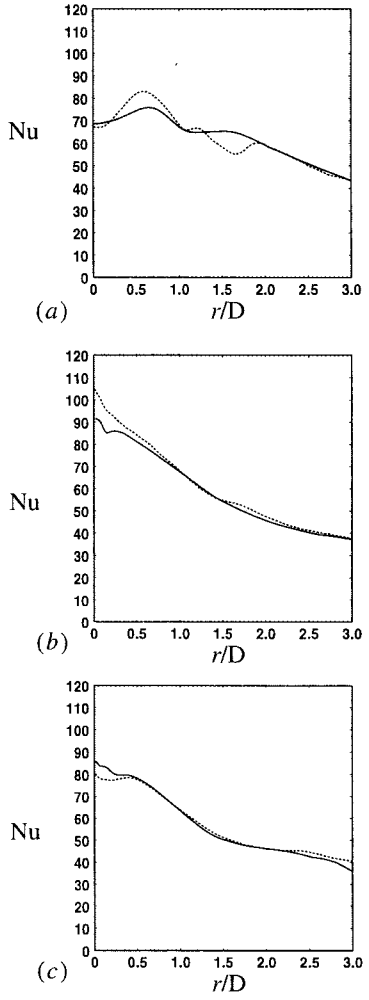

Figure 9: Nusselt number distributions along the impinging wall: (a) H/D = 2; (b) 6; (c) 10. ——, Without control; – – – – –, with control.

controlled case than that in the uncontrolled case.

Figure 7 shows the mean temperature (Θ_c) and rms temperature fluctuations (θ_{crms}) along the centerline in the controlled case, together with those in the uncontrolled case. As shown, the changes in the mean temperature and rms temperature fluctuations due to the excitation are similar to those observed for the axial velocity (Fig. 3).

Impinging jet

In the present study, three cases of H/D=2, 6 and 10 are considered. For each case, the same single frequency excitation at $St_\theta = 0.017$ is given to modify the mixing and heat transfer characteristics in the impinging jet. Figures 8(a), (b) and (c) show the instantaneous vortical structures without and with the excitation in the cases of H/D=2, 6 and 10, respectively. Here the vortical structures are identified by the iso-pressure. As shown in Fig. 8, vortical structures are very different for different H/D even without excitation. In other words, the existence of the impinging wall completely changes the initial development of jet flow. With the excitation, vortex rings are formed near the jet exit and develop in the downstream. However, the changes in the vortical structures by the excitation are different depending on H/D. In the cases of H/D = 2 and 6, the vortex

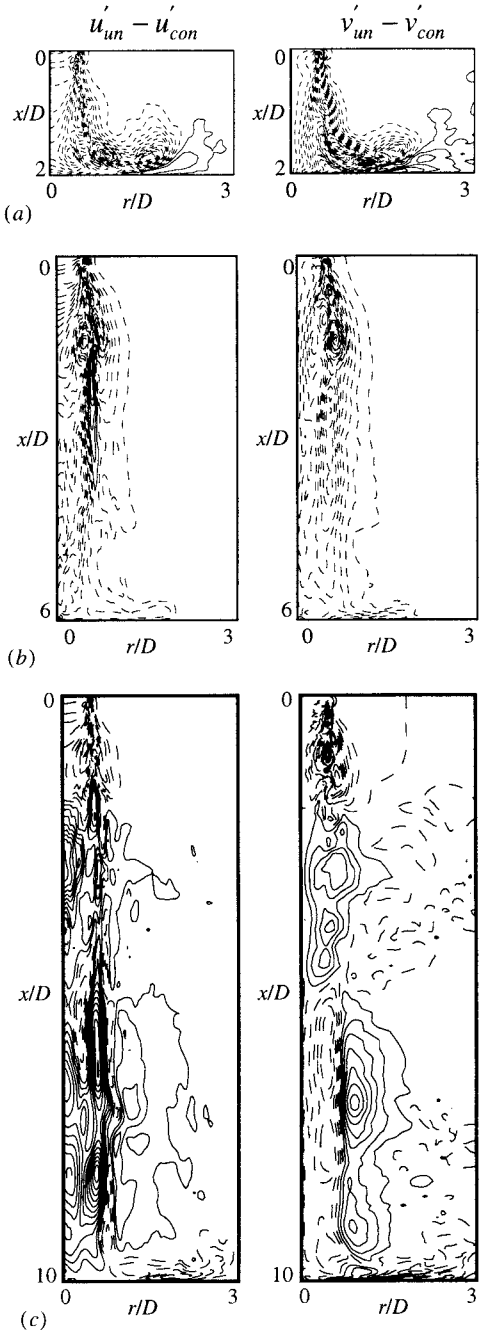

Figure 10: Changes in the Reynolds stresses due to the excitation: (a) H/D = 2; (b) 6; (c) 10. Contours of $u'_{un} - u'_{con}$ are (-0.37~0.06), (-0.20~0.10) and (-0.17~0.21) for (a), (b) and (c), respectively, and those of $v'_{un} - v'_{con}$ are (-0.28~0.10), (-0.35~0.01) and (-0.19~0.11) for (a), (b) and (c), respectively. Negative contours are dashed.

rings in downstream locations are larger than those in the uncontrolled case, whereas they are smaller in the case of H/D = 10. This behavior for H/D = 10 is similar to that observed in a downstream location of the free jet. The modification of vortical structures by the excitation is directly associated with the heat transfer rate on the wall.

Figure 9 shows the distributions of the Nusselt number at the impinging wall without and with the excitation. As expected from Fig. 8, the changes in the Nusselt number due to the excitation are very different depending on H/D. For H/D = 2, the excitation increases the Nusselt num-

ber near $r/D \sim 0.5$ but decreases it near $r/D \sim 1.5$. For $H/D = 6$, the excitation increases Nu for all r, especially near the stagnation region. For $H/D = 10$, the Nusselt number is reduced near the stagnation point by the excitation. This behavior for $H/D = 10$ is consistent with that of the free jet in which turbulence suppression is observed in a downstream location. However, the behaviors for $H/D = 2$ and 6 are very different from the expectation based on the free-jet excitation, and they seem to result from complicated interactions between the jet and impinging wall.

Figures 10(a), (b) and (c) show the changes in the axial and radial velocity fluctuations due to the excitation in the cases of $H/D = 2$, 6 and 10, respectively. The positive value (solid lines) indicates the region where turbulence suppression occurs due to the excitation. In the cases of $H/D = 2$ and 6, most regions have dashed lines, indicating that the turbulence intensities increase in most regions due to the excitation and therefore the Nusselt number increases in those regions (see Figs. 9(a) and (b)). This behavior is quite different from that observed in the free jet. On the other hand, for $H/D = 10$, the turbulence intensities increase in a downstream location of the jet exit and this behavior is similar to that observed from the free-jet excitation, indicating that the modification of flow variables by the excitation at $St_\theta = 0.017$ should be very sensitive to the downstream condition of the jet.

CONCLUSION

In the present study, we investigated an active control of turbulent free and impinging jets for mixing modification. As the active control, a single-frequency excitation was selected, and a non-dimensional frequency of $St_\theta = 0.017$ corresponding to the maximum growth rate in the mixing layer was selected as an excitation frequency. When the free jet was excited at $St_\theta = 0.017$, coherent structures broke down into fine-grained turbulence in the downstream, which significantly reduced turbulence there. Accordingly, the mixing in the controlled case was reduced as compared with that without excitation.

For the impinging jet, the changes in the Nusselt number due to the excitation significantly depended on H/D. The heat transfer rate near the stagnation region was increased in the cases of $H/D = 2$ and 6, whereas it was reduced in the case of $H/D = 10$. This enhancement resulted from the increase in the Reynolds stresses due to the excitation, but the decrease in the Nusselt number was due to the decrease in the Reynolds stresses due to the same excitation. This observation implies that the modification of flow variables by the excitation at $St_\theta = 0.017$ should be very sensitive to the downstream condition of the jet.

ACKNOWLEDGEMENT

This work is supported by the Creative Research Initiatives of the Korean Ministry of Science and Technology.

REFERENCES

Akselvoll, K., and Moin, P., 1995, "Large eddy simulation of turbulent confined coannular jets and turbulent flow over a backward facing step", *Report* No. TF-63, Department of Mechanical Engineering, Stanford University.

Crow, S. C., and Champagne, F. H., 1971, "Orderly structure in jet turbulence", *J. Fluid Mech.*, Vol 48, pp. 547-591.

Germano, M., and Piomelli, U., Moin, P., and Cabot, W. H., 1991, "A dynamic subgrid-scale eddy viscosity model", *Phys. Fluids* A, Vol. 3, pp. 1760-1765.

Ho, C-M., and Huerre, P., 1984, "Perturbed free shear layers", *Ann. Rev. Fluid Mech.*, Vol. 16, pp. 365-424.

Hwang, S. D., and Cho, H. H., 2003, "Effects of acoustic excitation positions on heat transfer and flow in axisymmetric impinging jet: main jet excitation and shear layer excitation", *Int. J. Heat Fluid Flow*, Vol. 24, pp. 199-209.

Koren, B., 1993, A robust upwind discretization method for advection, diffusion and source terms. In: vreugehill, C.B., Koren, B. (Eds.), Numerical methods for advection-diffusion problems. *Notes on Numerical Fluid Mechanics*, Vol. 45, Vieweg, Braunschweig, pp. 117-138.

Lee, J., and Lee, S. J., 1999, "Stagnation region heat transfer of a turbulent axisymmetric jet impingement", *Exp. Heat Transfer*, Vol. 12, pp. 137-156.

Lilly, D. K., 1992, "A proposed modification of the Germano subgrid-scale closure method", *Phys. Fluids* A, Vol. 4, pp. 633-635.

Liu, T., and Sullivan, J. P., 1996, "Heat transfer and flow structures in an excited circular impinging jet", *Int. J. Heat Mass Transfer*, Vol. 39, pp. 3695-3706.

Michalke, A., 1965, "On spatially growing disturbances in an inviscid shear layer", *J. Fluid Mech.*, Vol. 23, pp. 521-544.

Rajagopalan, S., and Antonia, R. A., 1998, "Turbulence reduction in the mixing layer of a plane jet using small cylinders", *Exp. Fluids*, Vol. 25, pp. 96-103.

Tong, C., and Warhaft, Z., 1994, "Turbulence suppression in a jet by means of a fine ring", *Phys. Fluids*, Vol. 6, pp. 328-333.

Zaman, K. B. M. Q., and Hussain, A. K. M. F., 1980, "Vortex pairing in a circular jet under controlled excitation. Part 1. General jet response", *J. Fluid Mech.*, Vol. 101, pp. 449-491 .

Zaman, K. B. M. Q., and Hussain, A. K. M. F., 1981, "Turbulence suppression in free shear flows by controlled excitation", *J. Fluid Mech.*, Vol. 103, pp. 133-159.